

#### Research Article

# Impact of Die Exit Temperature on the Crystalline Orientation and Performance of Polypropylene Battery Separators

Panalee Kerdthong School of Science, Mae Fah Luang University, Chiang Rai, Thailand

Sitthi Duangphet\*, Nattakan Soykeabkaew and Uraiwan Intatha Center of Innovative Materials for Sustainability (iMatS), Mae Fah Luang University, Chiang Rai, Thailand

Nuntaporn Kamonsutthipaijit and Sukanya Tastub Synchrotron Light Research Institute (Public Organization), Nakhon Ratchasima, Thailand

\* Corresponding author. E-mail: sitthi.dua@mfu.ac.th DOI: 10.14416/j.asep.2025.10.002 Received: 18 June 2025; Revised: 24 July 2025; Accepted: 29 August 2025; Published online: 8 October 2025 © 2025 King Mongkut's University of Technology North Bangkok. All Rights Reserved.

#### Abstract

Lithium-ion battery separators play a crucial role in ensuring the efficiency and safety of modern energy storage systems. The melt-stretching method is commonly used for polypropylene battery separator fabrication, with research extensively exploring how extrusion parameters influence the final product's structure and properties. However, the specific impact of die exit temperature on separator quality remains largely unexamined. This study investigates the effect of die exit temperature during the dry process on the performance of polypropylene microporous membranes used as battery separators. Separators were produced using a co-rotational twin-screw extruder at various die exit temperatures (215–245 °C) and characterized for their crystalline orientation, porosity, and battery performance. Polarized FTIR and 2D-WAXS analyses revealed that lower die exit temperatures improve crystalline orientation, resulting in more uniform pore structures. At 215 °C, the separators exhibited superior electrolyte uptake (109.4%) and better pore morphology. The coin cell tests revealed that separators fabricated at 215 °C achieved higher charge storage capacity (181.45 mAh) and greater efficiency compared to those produced at elevated temperatures. These findings underscore the critical role of optimizing die exit temperature in the production of high-performance battery separators.

**Keywords**: Die exit temperature, Dry process, Lithium-ion battery, Polypropylene, Separator

#### 1 Introduction

Lithium-ion batteries (LIBs) have become indispensable in modern energy storage solutions, driving advancements in a wide range of technologies, from portable electronic devices to electric vehicles (EVs) and large-scale renewable energy systems. Their superior energy density, long cycle life, and low self-discharge rates make them essential in both consumer and industrial applications [1]. A lot of research has focused on the anode, cathode, and electrolyte of LIBs, but the often-overlooked battery separator is now recognized as a

vital component for improving performance and safety of LIBs.

A separator in a lithium-ion battery is a thin, microporous membrane positioned between the anode and cathode to prevent direct contact between these electrodes, thus avoiding short circuits and potential thermal runaway events, which could lead to dangerous failures like fires or explosions [2]. Besides acting as a physical barrier, the separator must allow the free flow of lithium ions during the charging and discharging cycles to ensure the battery operates efficiently. Therefore, the separator directly influences



key battery attributes, including performance, longevity, and safety [3].

The demands placed on lithium-ion batteries are continually increasing, particularly in high-performance applications such as EVs and grid energy storage, where efficiency, durability, and safety are paramount [4]. As a result, there is growing pressure to optimize separator materials and manufacturing processes. While separators must offer high ionic conductivity to facilitate ion transport, they must also exhibit robust mechanical strength, thermal stability, and chemical resistance to withstand the physical and thermal stresses encountered during battery operation. Two primary manufacturing methods dominate production of separators: the wet process and the dry process. The wet process is solvent-based, offering precise control over separator thickness and porosity but posing environmental challenges and higher production costs [5]. In contrast, the dry process, which relies on the melt extrusion of crystalline polymers, is more cost-effective and environmentally friendly. However, the dry process is restricted to a limited range of polymers, [6] primarily polypropylene (PP) and polyethylene (PE), which may not offer the full spectrum of desirable properties, such as flexibility and enhanced ionic conductivity.

The quality of polypropylene microporous membranes used as battery separators is heavily influenced by key processing parameters such as annealing, stretching, and the addition of fillers [7]. The process starts by extruding PP at a high die draw ratio (DDR) to generate a high crystalline orientation (row-like lamellae) film. Annealing improves lamellae periodicity and crystallinity, which enhances mechanical strength and stability. The film stretching process, particularly cold and hot stretching, is critical for pore formation, with hot stretching further separating lamellae to create stable pores. Additives like nano-SiO<sub>2</sub> (at 2%) enhance tensile strength without compromising pore structure, magnesium sulfate whiskers improve strength along the transverse direction and electrolyte absorption [8]. Proper control of the chill roll temperature and stretching ratios is crucial for optimizing porosity, mechanical integrity, and thermal stability. All of them are essential for producing high-performance battery separators.

The extrusion parameters during the melt extrusion of precursor films are key factors that affect the performance of battery separators. The effect of DDR, chill roll temperature, and assistance of air-

cooling [9]–[11] on separator performance is usually reported. However, no study has yet explained the relationship between the die exit temperature and the quality of the battery separator. In every previous research, the die exit temperature is only mentioned at a specific value without further explanation.

This study aims to explore the relationship between die exit temperatures and the quality of lithium-ion battery separators produced through the dry process, so that their quality can be controlled beforehand rather than depending entirely on post-processing changes. The impact of various die exit temperatures on the crystallization of precursor film and separator was investigated using polarized Fourier Transform Infrared Spectroscopy (FTIR), two-dimensional wide-angle X-ray scattering, and scanning electron microscopy. Furthermore, the key properties of the prepared separator, such as electrolyte uptake and thermal shrinkage, as well as the performance of assembled coin-type lithium-ion batteries, were assessed.

#### 2 Materials and Methods

# 2.1 Materials

Commercial-grade Polypropylene was supplied by Sinopec (PPH-T03-S) with a density of 0.905 g/cm<sup>-3</sup> (under ASTM D 792) and a melt flow rate of 2.46 g/10 min (under ASTM D 1238 at 230 °C and 2.16 kg). The melting point (Tm) and crystallinity obtained from DSC (Model Q2000 TA Instrument) at the rate of 10 °C/min were 166.1 °C and 49.4% respectively. The molecular weight measured using GPC-IR Polymer Char's was 374,500 g/mol.

# 2.2 Sample preparation

# 2.2.1 Preparation of precursor film

The precursor films were produced using a corotational twin-screw extruder (Collin Compounder ZK 25 E, Germany) connected with a coated hanger die (30 cm). The temperature profile started from room temperature at the hopper and gradually increased to 245 °C in the final zone prior to die exit. The temperature of the extrusion die was adjusted between 215 and 245 °C. In this study, 215 °C was the lowest temperature at which the film could still be produced and temperatures lower than 215 °C resulted in blockage at the die exit of the extruder. An air knife



(Chareontut Co. Ltd., Thailand) was installed to supply air to the film surface right at the exit of the die. After being extruded from the die, the molten polymer film was collected with the chill roll (Collin Chill-Roll 144/350, Germany). The temperature of the first roll of the chill roll was set at 90 °C and die draw ratios (DDR) of 140, 160 and 180 were applied. In this study, DDR higher than 180 did not produce precursor film due to film tearing, while under 140 DDR, no crystalline orientation could be observed. The precursor films were subsequently annealed at 145 °C for 30 min to enhance the crystalline structure in order to make it easier for micropores to grow during the next stretching stage.

# 2.2.2 Microporous membrane preparation

The annealed films were cut to a width of 25 mm and a length of 100 mm for cold and hot stretching, which was operated using the universal testing machine (Instron 5566, USA) equipped with the temperature-controlled chamber (Instron, USA). The distance between the grips was set at 50 mm. The films were stretched uniaxially along the machine direction (MD) at 25 and 130 °C for cold and hot stretching, respectively. The stretching rate was set at 50 mm/min for both cold and hot stretching. The stretching ratio of cold stretching was 20% while the hot stretching was 100%. Finally, the stretched films were thermally set at 145 °C for a duration of 10 min.

# 2.3 Preparation of electrode

The CR2032 coin-cell configuration was utilized for electrochemical tests. The working electrode was prepared by mixing 98 wt% porous carbon material, 1 wt% acetylene black, and 1 wt% polyvinylidene fluoride (PVDF) as a binder. This mixture was then dispersed in N-methyl-2-pyrrolidone (NMP) solution to form a slurry. The slurry was uniformly cast onto copper foil using a blading machine to control the thickness and subsequently dried in a vacuum oven at 120 °C for less than 12 h. The separator was added, and the assembly of the coin cells was performed in an argon-filled glove box, with a lithium metal chip serving as the counter electrode and 1 mol/L LiPF<sub>6</sub> solution as the electrolyte.

#### 2.4 Characterizations

#### 2.4.1 Polarized Fourier transform infrared spectroscopy

The crystalline orientation of precursor film was determined by polarized FTIR using a Bruker Tensor 27 Infrared Spectrometer connected to a Bruker Hyperion 3000 Infrared Microscope. The sample was positioned in the path of the polarized beam, and spectra were obtained for both parallel and perpendicular polarizations in relation to the melt extrusion orientation. The OPUS 7.5 software (Bruker Optic Ltd, Ettlingen, Germany) was employed to analyze the results. The FTIR spectra were recorded at room temperature by using 4 cm<sup>-1</sup> resolution and 64 scans over a measurement spectrum from 4,000 to 400 cm<sup>-1</sup>. The crystalline orientation factor (F<sub>c</sub>) was calculated based on the resulting data, which delivers information regarding the degree of alignment of the polymer chains within the film. [12].

The Herman orientation function (F) can be calculated from Equation (1):

$$F = \frac{D-1}{D+2} \tag{1}$$

The dichroic ratio, D, is determined by the following Equation (2):

$$D = \frac{A_{\parallel}}{A_{\perp}} \tag{2}$$

Where  $A_{\parallel}$  denotes the absorption parallel and  $A_{\perp}$  the absorption perpendicular to a specific reference axis [13].

Absorption at a wavenumber of 998 cm<sup>-1</sup> is associated with the crystalline phase (c-axis) in polypropylene, while absorption at 972 cm<sup>-1</sup> involves both crystalline and amorphous phases. The crystalline orientation factor (F<sub>c</sub>) can be determined from the former absorption, whereas the latter provides the average orientation function (F<sub>am</sub>). These values can be used to determine the orientation of the amorphous phase (F<sub>am</sub>) by the following Equation (3).

$$F_{av} = X_c F_c + (1 - X_c) F_{am} (3)$$

where X<sub>c</sub> represents the degree of crystallinity.



## 2.4.2 Two-dimensional wide-angle X-ray scattering

The crystalline structure and orientation of precursor film at the atomic and molecular levels are investigated using two-dimensional wide-angle X-ray scattering (2D-WAXS). The 2D-WAXS was conducted at the Synchrotron Light Research Institute in Thailand using a Beamline 1.3W equipped with an SX165 CCD detector. The data is accumulated for 300 s and collected with an X-ray energy of 9 keV.

### 2.4.3 Scanning electron microscopy

The surface morphology and microstructure of separators were visualized using a Scanning Electron Microscope (Tescan, Mira). All samples without further treatment were cut into 5 mm × 5 mm and then coated with gold by sputtering. A focused electron beam is traversed over the surface of the sample using an accelerating voltage of 5 keV.

# 2.4.4 Electrolyte uptake

Electrolyte uptake was obtained by immersing the separator in a liquid electrolyte of 1.0 M LiPF<sub>6</sub> in EC/DEC = 50/50 (v/v), battery grade, for 2 h. The separator electrolyte uptake was determined using the formula (4):

*Uptake* % = 
$$\frac{W_2 - W_1}{W_2} \times 100$$
 (4)

where  $W_1$  and  $W_2$  represent the weight of the dry and wet separator, respectively [14].

#### 2.4.5 Thermal shrinkage

The separator was placed in an oven and heated to 90 °C for 1 h [15] to examine its thermal shrinkage behavior. The thermal shrinkage of the separator was calculated using the formula (5):

Shrinkage 
$$\% = \frac{S_0 - S_1}{S_0} \times 100$$
 (5)

where the separator area after and before thermal treatment is denoted as  $S_1$  and  $S_0$ , respectively, [16].

#### 2.4.6 Pore size

The pore size of the separator needs to be sufficiently small compared to the particle size of the electrode components. In real-world applications, submicrometer pore sizes have demonstrated their effectiveness in preventing internal short circuits by obstructing the entry of larger electrode particles or lithium dendrites [17]. The pore size of the separator was evaluated using ImageJ software. Statistical analysis of 100 pores on SEM images provided average pore size (length) data.

# 2.4.7 Battery performance

The performance of the lithium-ion batteries was evaluated using a Neware BST4000 battery testing system, integrated with BTS7.6.x software from China. This system enables precise control and real-time monitoring of charge-discharge cycles. The batteries underwent a series of charge-discharge cycles in constant current (CC) and constant voltage (CV) modes to evaluate key performance metrics, including capacity retention, energy efficiency, and cycle life.

#### 3 Results and Discussion

# 3.1 The effect of the die exit temperature on the crystal orientation of precursor film and separator morphology

During the precursor film preparation, die draw ratio (DDR) and die exit temperature play an important role in affecting crystallization structure. In terms of DDR, the extruded film is drawn by the chilled roll, which controls the DDR, then the lamellar structure shifts from spherulitic to more oriented row structure [10], [18]. From our preliminary observations, the oriented row structure was first observed at 140 DDR. Below this DDR, the oriented row structure cannot be detected. Due to the limitation of chilled roll speed, the maximum DDR was set at 180.

In this study, the die exit temperature was observed between 215–245 °C. Theoretically, a decrease in the die exit temperature results in faster cooling of the film. However, if the temperature is too low, it can negatively affect the film's surface quality, causing the solidified polymer to accumulate at the die exit, leading to uneven film thickness and rough surfaces. If the temperature drops too low, it may even cause blockages at the die exit. In this study, 215 °C is the lowest temperature at which film production was still possible. The effect of die exit temperature on the crystalline orientation factor (F<sub>c</sub>) of precursor films



was characterized by the polarized FTIR technique, as shown in Figure 1.

From Figure 1, the die exit temperature and DDR notably affect the F<sub>c</sub>. The F<sub>c</sub> values using the die exit temperature 215 °C are not involved by DDR. When the die exit temperature increases, the precursor film produced from 140 DDR presented a significant drop in F<sub>c</sub>. For precursor films produced from 160 and 180 DDR, the die exit temperature has no considerable effect on F<sub>c</sub> values. Moreover, it is clearly observed that the film produced from 160 DDR provided a higher F<sub>c</sub> than 180 DDR in every die exit temperature. This reduction decreases because the excessive drawing speed damages the lamellae [19]. This result suggests that 160 DDR is a suitable parameter in this study.

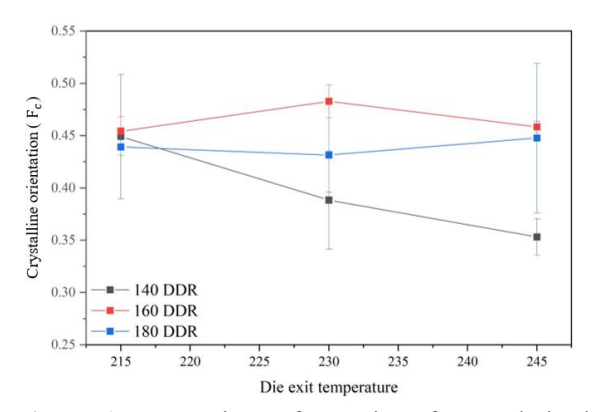


**Figure 1**: Comparison of F<sub>c</sub> values from polarized FTIR of precursor films prepared at different die exit temperatures using a DDR range of 140–180.

Our findings align with those reported by Xu et al. [19], who investigated how the die draw ratios (DDR) influence the crystalline orientation of polypropylene (PP) films, focusing on DDR values between 20 and 170. Their analysis utilized polarized FTIR and WAXD techniques. Results from polarized FTIR indicated that crystalline orientation improved with increasing DDR. However, at 170 DDR, crystalline orientation diminished as it reached a critical limit. This observation was corroborated by WAXD data, which showed a reduction in circularity at DDR 170.

This research observed the 2D-WAXS and our polarized FTIR results are consistent with the 2D-WAXS results shown in Figure 2. Generally, the 2D-WAXS pattern of spherulitic crystalline PP presents the ring formation on 110, 040, 130 and 111 planes [20]. The increase in crystalline orientation transforms the ring into an arc formation. The shorter the length

of the arc, the higher the degree of crystalline orientation [11]. In comparison between the die exit temperatures of 215 °C to 245 °C, the 2D-WAXS patterns obviously show the change from ring to arc formation. Figure 2 clearly shows that the diffraction rings remain nearly complete at a die exit temperature of 245 °C, and the ring circularity decreases as the temperature drops. Moreover, the 2D-WAXS result also confirmed that 160 DDR is a suitable parameter to produce precursor film due to short arc formation. Therefore, 160 DDR was selected for further separator properties and battery performance tests.

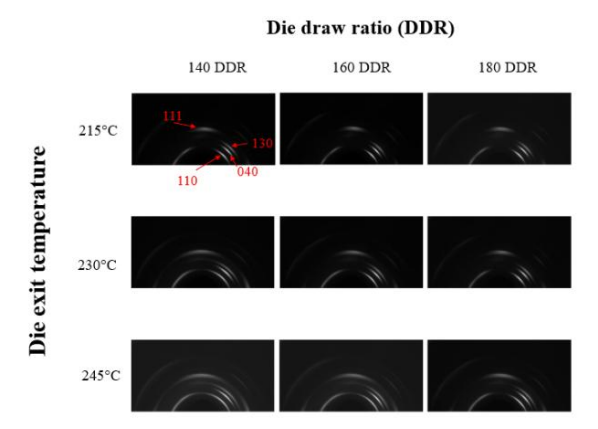


**Figure 2**: The 2D-WAXS patterns of precursor films prepared at different die exit temperatures using a DDR range of 140–180.

The die exit temperature was a key parameter on shear-induced crystalline of isotactic polypropylene (iPP). Farah and Bretas [21] demonstrated the shearinduced crystallization of iPP in a slit die using a temperature range 169-230 °C and found that the shear-induced crystalline was particularly established near the die wall, where the shear rate is the highest and the thickness of the shear-induced crystalline layer increased at lower die temperature (T<sub>d</sub>). At low die temperatures, such as 169 °C, the cooling rate is high, allowing the polymer melt to crystallize more rapidly under shear. Additionally, at these low temperatures, the thickness of the crystalline layer increased along the length of the die due to the prolonged exposure to shear, which facilitated continued crystallization. In contrast, at higher die temperatures, such as 200 °C or above, the crystallization process was significantly delayed due to reduced undercooling. The polymer remained in a molten state for a longer time, limiting the alignment and crystallization of the polymer chains. This led to thinner crystalline layers or, in some



cases, the absence of shear-induced crystallization. These findings underline that lower die temperatures favor the formation of shear-induced crystalline layers, while higher temperatures suppress this effect, emphasizing the importance of thermal conditions in extrusion processes. The effect of temperature on the formation of nuclei was also explored. Bednarek *et al.*, [22] found that low temperatures and shear enhance nucleation density and stabilize  $\alpha$ - and  $\beta$ -phase nuclei in iPP. Lower temperatures favor  $\beta$ -phase formation (row-like lamellae) while higher temperatures favor  $\alpha$ -phase formation (spherulite) as chain relaxation dominates, reducing  $\beta$ -phase stability.

To investigate the effect of crystalline orientation on micropore formation in the separator at different die exit temperatures, the SEM technique was used, and the image of the separator was produced from precursor films that were formed under different conditions, are shown in Figure 3.

The SEM images in Figure 3 showed the porosity morphology of the separator produced from various die exit temperatures. It is evidenced to show that the separation of the lamellae structure during hot and cold stretching generated the pore morphology. For a separator produced from a die exit temperature 215 °C,

the pore size is more oriented and uniform. But when the die exit temperature increases, twisted lamellae structures and non-uniform pores are observed and some areas present closed pores, which reduces porosity efficiency.

It is noticed that the high crystalline orientation precursor film offers good and uniform pore size. Xu et al., [11] investigated the effect of melt-draw ratio (MDR) on the crystalline orientation and porosity of polypropylene membranes, focusing on the structural evolution and its impact on membrane performance and found a strong correlation between MDR, crystalline orientation, and porosity. As the MDR increased, crystalline orientation improved significantly. This enhancement in orientation refined the lamellar structure and reduced defects, resulting in increased porosity. So, it is suggested that higher crystalline orientation leads to greater porosity. In this study, both the die exit temperature and DDR influence the crystalline orientation, which in turn affects the quality of the porosity. Reducing the die exit temperature promotes the formation of more nuclei, resulting in a higher crystalline orientation, leading to better pore morphology.

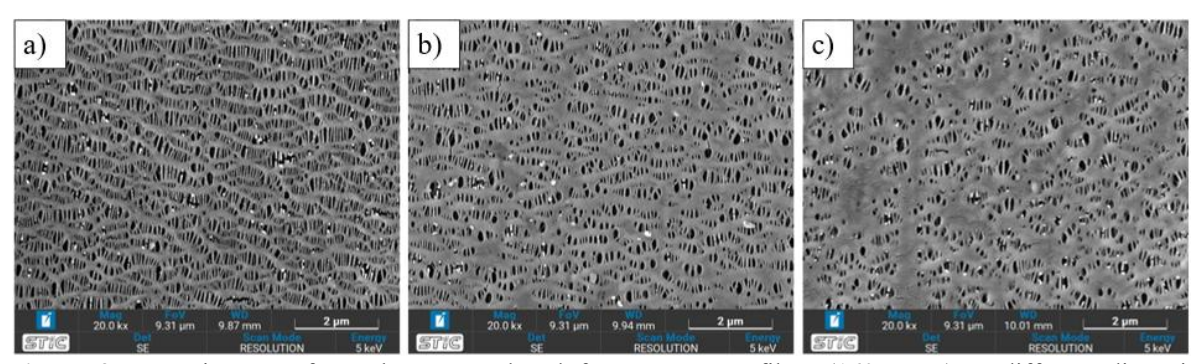


**Figure 3**: SEM images of membranes produced from precursor films (160 DDR) at different die exit temperatures: a) 215 °C, b) 230 °C, c) 245 °C.

**Table 1**: Comparison of separator performance. The separators are produced from precursor films (160 DDR) at different die exit temperatures.

No.	Sample	Pore Size (µm)	Shrinkage (%)	Electrolyte Uptake (%)
1	215 °C	$0.265 \pm 0.066$	$5.8 \pm 3.5$	$109.4 \pm 4.4$
2	230 °C	$0.236 \pm 0.070$	$2.0 \pm 2.9$	$88.2 \pm 16.6$
3	245 °C	$0.197 \pm 0.051$	$2.8 \pm 2.7$	$41.0 \pm 8.0$

# 3.2 The effect of the die exit temperature on the performance of separators

The data in Table 1 illustrate the effect of die exit temperature on the pore size, shrinkage, and

electrolyte uptake of separators. As the die exit temperature increases from 215 °C to 245 °C, the pore size and electrolyte uptake decrease, while the shrinkage percentages remain relatively low. At 215 °C, the separator demonstrates the largest average pore



size (0.265  $\pm$  0.066  $\mu$ m) and the highest electrolyte uptake (109.4  $\pm$  4.4%). However, as the temperature rises to 230 °C and 245 °C, the average pore sizes shrink to 0.236  $\pm$  0.070  $\mu$ m and 0.197  $\pm$ 0.051  $\mu$ m, respectively. Correspondingly, the electrolyte uptake drops significantly to 88.2  $\pm$  16.6% and 41.0  $\pm$  8.0%. The observed trend suggests that higher die exit temperatures lead to collapsed pore structures, reducing the separator's ability to absorb electrolytes.

Electrolyte uptake reflects the separator's ability to retain liquid electrolyte, which plays a critical role in supporting the electrochemical processes within the battery. The correlation between pore size and electrolyte uptake is evident, as smaller pore sizes at higher temperatures reduce the space for electrolyte retention. This finding aligns with Zhang et. al., [23] research, the study developed a nano-composite polymer electrolyte membrane (NCPE) by integrating a highly dispersed nano-TiO<sub>2</sub> hybrid with PVDF-HFP into glass fiber nonwoven, achieving a porosity of 58%, significantly higher than conventional PP separators 38%. This increased porosity enabled the NCPE to absorb 330% liquid electrolyte, compared to 55% for PP, highlighting a direct relationship between porosity and electrolyte uptake. Where separators with high porosity and interconnected pores demonstrate better electrolyte wettability and Additionally, electrolyte uptake can serve as an indirect measure of separator porosity, quantifying the liquid absorbed into the pores, a commonly used method in battery material research [24].

Table 2 summarizes the charge and discharge characteristics of coin-type CR2032 half-cells using

separators processed at varying die exit temperatures (215 °C, 230 °C, and 245 °C). These separators were tested under a voltage range of 3.0–4.2 V with a charge density (C-rate) of 0.1C. Among the tested separators, the one processed at 215 °C demonstrated superior performance with the highest specific capacities during charging (181.45 mAh/g) and discharging (178.74 mAh/g) and an impressive charge/discharge efficiency of 98.51%. The corresponding cell capacity was 2.30 mAh, with the cell maintaining stability for 21 cycles.

By comparison, commercial lithium-ion batteries typically achieve specific capacities ranging from 140 to 170 mAh/g for cathode materials such as LiCoO<sub>2</sub> and LiNiMnCoO<sub>2</sub> at similar C-rates [25]. This suggests that the separator processed at 215 °C performs competitively in terms of specific capacity, while its efficiency exceeds that of many commercial often exhibit charge/discharge which efficiencies between 95% and 98% due to electrolyte degradation and electrode polarization.

The separator processed at 230 °C, however, exhibited drastically reduced performance, with specific capacities of 44.75 mAh/g (charge) and 52.21 mAh/g (discharge), and a charge/discharge efficiency of only 85.71%. Despite this, it demonstrated better cycle life, sustaining over 50 cycles. Commercial lithium-ion batteries often achieve cycle lives exceeding 500–1000 cycles under similar conditions, highlighting the importance of further optimizing separator properties and ensuring compatibility with electrodes to extend cycle life without compromising capacity.

**Table 2**: Shows the values of charge and discharge testing for coin-type batteries. CR2032 half-cell uses a voltage range of 3.0–4.2 V and a charge density (C-rate) of 0.1C

No.	Sample	Specific Capacity Charge (mAh/g)	Specific Capacity Discharge (mAh/g)	Chg/Dchg Efficiency (%)	Capacity (mAh)	Battery Cycle
1	215 °C	181.45	178.74	98.51	2.30	21
2	230 °C	44.75	52.21	85.71	0.62	>50
3	245 °C	84.751	97.73	86.72	1.16	32

The separator processed at 245 °C achieved moderate improvements over the 230 °C sample, with specific capacities of 84.75 mAh/g (charge) and 97.73 mAh/g (discharge) and a charge/discharge efficiency of 86.72%. However, it remained below the performance of both the 215 °C separator and commercial separators, which generally provide stable performance with minimal polarization over several hundred cycles.

Figure 4 shows the galvanostatic charge-discharge profiles for separators processed at different die exit temperatures. The separator processed at 215  $^{\circ}\text{C}$  displayed the highest specific capacity (~180 mAh/g) and a stable voltage plateau, indicative of efficient lithium intercalation and deintercalation. Its excellent performance is attributed to superior electrolyte uptake (109.4  $\pm$  4.4%) and a larger pore size (0.265  $\pm$  0.066  $\mu m$ ), enhancing ionic conductivity and reducing polarization. These characteristics make



it comparable to commercial polypropylene or polyethylene separators, which feature high porosity and uniform pore structures to maximize ionic transport.

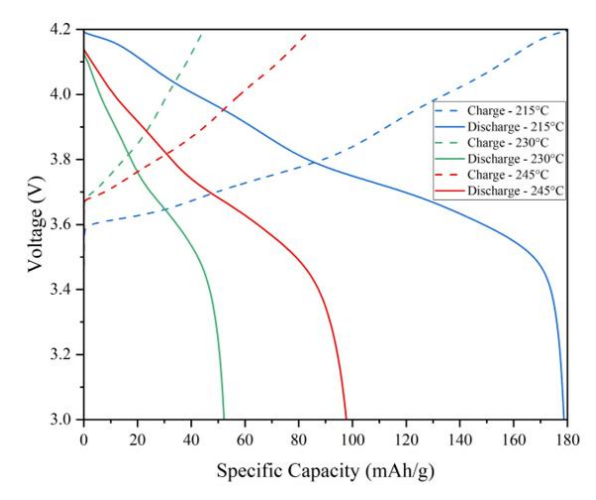


**Figure 4**: Galvanostatic Charge-Discharge profile of separators from coin-type batteries. CR2032 half-cell uses a voltage range of 3.0–4.2 V and a charge density (C-rate) of 0.1 C.

In contrast, the separator processed at 230 °C exhibited significant limitations, with reduced specific capacity (~50 mAh/g) and irregular voltage profiles. Lower electrolyte uptake (88.2  $\pm$  16.6%) and smaller pore size (0.236  $\pm$  0.070  $\mu m$ ) contributed to increased resistance and restricted lithium-ion mobility. Such limitations are less common in commercial separators, which are engineered for consistent porosity and superior electrolyte compatibility.

The separator processed at 245 °C demonstrated intermediate performance, with specific capacity (~90 mAh/g) higher than the 230 °C sample but much lower than both the 215 °C sample and commercial counterparts. Its smaller pore size (0.197  $\pm$  0.051  $\mu m$ ) and significantly reduced electrolyte uptake (41.0  $\pm$  8.0%) limited its ability to support efficient ionic transport, causing steep polarization and efficiency loss. Commercial separators generally avoid these issues by employing controlled thermal and mechanical processing to achieve optimized structural properties.

These results align with Kim *et al.* [24], who emphasized that high porosity and superior electrolyte uptake are critical for enhanced ionic conductivity and se cycling performance. Their findings showed that protonated TOCN membranes (TOCN-COOH) achieved 94.5% capacity retention after 100 cycles,

outperforming their sodium carboxylated counterparts (TOCN-COO<sup>-</sup>Na<sup>+</sup>). The superior performance of these membranes highlights the importance of optimized separator properties for competitive battery performance.

In summary, the separator processed at 215 °C demonstrated performance on par with commercial lithium-ion battery separators in terms of specific capacity and charge/discharge efficiency, though further improvements are required to match the extended cycle life and broader compatibility of commercial options. These findings underline the importance of precisely controlling thermal processing conditions during separator fabrication to achieve the structural and electrochemical properties necessary for high-performance lithium-ion batteries.

#### 4 Conclusions

In this study, the polypropylene battery separators were fabricated via a dry process with different die exit temperatures, a parameter often overlooked in separator fabrication. Fine-tuning this temperature directly influences crystalline orientation and pore development, which in turn affects electrolyte affinity and overall electrochemical behavior. Lower die temperatures considerably promote the formation of more ordered lamellar structures and interconnected pores, offering significant improvements in separator functionality. This study underlines the importance of optimizing thermal conditions during precursor film manufacturing as a strategic approach to improving separator performance, rather than relying solely on post-processing modifications. Future studies should transition the optimal die temperature conditions from the laboratory to pilot-scale manufacturing to validate industrial feasibility and expand the material scope to include polyethylene (PE) or PP/PE blends. Furthermore, combining this optimized thermal process with functional additives and subjecting the separators to advanced, long-term resulting electrochemical and safety testing would clarify their potential for high-performance commercial applications.

### Acknowledgments

This research was financially supported by Mae Fah Luang University, National Research Council of Thailand (NRCT) and National Science, Research and Innovation Fund (NSRF) (Grant no. N23D650045). The authors would like to express their heartfelt



gratitude to IRPC Public Company Limited, Thailand for their generous support in providing access to machinery, equipment, and testing facilities, as well as their invaluable technical assistance throughout this study. Additionally, we extend our special thanks to the Synchrotron Light Research Institute (Public Organization), Thailand for granting access to their facilities and providing critical support for the 2D-WAXS analysis. The authors also would like to thank Electro-Ceramics Research Laboratory, Faculty of Science, Chiang Mai University, Thailand for their support and collaboration throughout the research process.

#### **Author Contributions**

P.K.: research design, investigation, reviewing, methodology, data collection, writing, data analysis and editing; S.D.: conceptualization, research design, investigation, reviewing, methodology, writing, data analysis, funding acquisition and editing; N.S.: research design, data analysis and editing; U.I.: conceptualization, research design, methodology, data analysis, administration, funding acquisition and editing; N.K.: methodology, investigation, data collection; S.T.: methodology, investigation, data collection. All authors have read and agreed to the published version of the manuscript.

# **Conflicts of Interest**

The authors declare no conflict of interest.

# References

- [1] C. Shunhong, S. Pullteap, and T. Mao, "Research progress and future expectations in anode of secondary zinc-air batteries: A review," *Applied Science and Engineering Progress*, vol. 17, no. 3, Jul. 2024, Art no. 7410, doi: 10.14416/j.asep. 2024.06.006.
- [2] M. Lowe, S. Tokuoka, T. Trigg, and G. Gereffi, "Lithium-ion batteries for electric vehicles: the U.S. value chain," Duke University CGGC: Durham, NC, USA, Oct. 2010, doi: 10.13140/RG.2.1.1421.0324.
- [3] S. Mahmud et al., "Recent advances in lithiumion battery materials for improved electrochemical performance: A review," *Results in Engineering*, vol. 15, Sep. 2022, Art no. 100472, doi: 10.1016/j.rineng.2022.100472.

- [4] N. Lingappan, W. Lee, S. Passerini, and M. Pecht, "A comprehensive review of separator membranes in lithium-ion batteries," *Renewable and Sustainable Energy Reviews*, vol. 187, Nov. 2023, Art. no. 113726, doi: 10.1016/j.rser.2023. 113726.
- [5] P. Arora and Z. Zhang, "Battery separators," *Chemical Reviews*, vol. 104, no. 10, pp. 4419–4462, Oct. 2004, doi: 10.1021/cr020738u.
- [6] S. S. Zhang, "A review on the separators of liquid electrolyte Li-ion batteries," *Journal of Power Sources*, vol. 164, no. 1, pp. 351–364, Jan. 2007, doi: 10.1016/j.jpowsour.2006.10.065.
- [7] M. Yang and J. Hou, "Membranes in lithium ion batteries," *Membranes*, vol. 2, no. 3, pp. 367–383, Jul. 2012, doi: 10.3390/membranes2030367.
- [8] C. Lei, Q. Cai, R. Xu, X. Chen, and J. Xie, "Influence of magnesium sulfate whiskers on the structure and properties of melt-stretching polypropylene microporous membranes," *Journal of Applied Polymer Science*, vol. 133, no. 35, Sep. 2016, Art no. 43884, doi: 10.1002/app.43884.
- [9] Y. Lin et al., "A semi-quantitative deformation model for pore formation in isotactic polypropylene microporous membrane," *Polymer*, vol. 80, pp. 214–227, Dec. 2015, doi: 10.1016/j.polymer.2015.10.067.
- [10] S. H. Tabatabaei, P. J. Carreau, and A. Ajji, "Effect of processing on the crystalline orientation, morphology, and mechanical properties of polypropylene cast films and microporous membrane formation," *Polymer*, vol. 50, no. 17, pp. 4228–4240, Aug. 2009, doi: 10.1016/j.polymer.2009.06.071.
- [11] R. Xu, X. Chen, J. Xie, Q. Cai, and C. Lei, "Influence of melt-draw ratio on the crystalline structure and properties of polypropylene cast film and stretched microporous membrane," *Industrial & Engineering Chemistry Research*, vol. 54, no. 11, pp. 2991–2999, Mar. 2015, doi: 10.1021/acs.iecr.5b00215.
- [12] L. Ding, R. Xu, L. Pu, F. Yang, T. Wu, and M. Xiang, "Pore formation and evolution mechanism during biaxial stretching of β-iPP used for lithium-ion batteries separator," *Materials and Design*, vol. 179, Oct. 2019, Art no. 107880, doi: 10.1016/j.matdes.2019.107880.
- [13] Y. Ren, H. Zou, S. Wang, J. Liu, D. Gao, C. Wu, and S. Zhang, "Effect of annealing on microstructure and tensile properties of polypropylene cast film,"



- Colloid and Polymer Science, vol. 296, no. 1, pp. 41–51, Jan. 2018, doi: 10.1007/s00396-017-4220-8.
- [14] J. Cui, J. Liu, C. He, J. Li, and X. Wu, "Composite of polyvinylidene fluoride–cellulose acetate with Al(OH)<sub>3</sub> as a separator for high-performance lithium ion battery," *Journal of Membrane Science*, vol. 541, pp. 661–667, Nov. 2017, doi: 10.1016/j.memsci.2017.07.048.
- [15] V. Deimede and C. Elmasides, "Separators for lithium-ion batteries: A review on the production processes and recent developments," *Energy Technology*, vol. 3, no. 5, pp. 453–468, May. 2015, doi: 10.1002/ente.201402215.
- [16] Y. Li, H. Pu, and Y. Wei, "Polypropylene/polyethylene multilayer separators with enhanced thermal stability for lithium-ion battery via multilayer coextrusion," *Electrochimica Acta*, vol. 264, pp. 140–149, Feb. 2018, doi: 10.1016/i.electacta.2018.01.114.
- [17] H. Lee, M. Yanilmaz, O. Toprakci, K. Fu, and X. Zhang, "A review of recent developments in membrane separators for rechargeable lithiumion batteries," *Energy & Environmental Science*, vol. 7, no. 12, pp. 3857–3886, Dec. 2014, doi: 10.1039/c4ee01432d.
- [18] C. Li and R. Xu, "Melt-stretching polyolefin microporous membrane," in *Submicron Porous Materials*, P. Bettotti, Ed. Cham: Springer, 2017, pp. 81–105. doi: 10.1007/978-3-319-53035-2\_4.
- [19] R. Xu, S. Zeng, J. Wang, J. Kang, M. Xiang, and F. Yang, "Impact of different die draw ratio on crystalline and oriented properties of polypropylene cast films and annealed films," *Journal of Polymer Research*, vol. 25, May.

- 2018, Art. no. 142 doi: 10.1007/s10965-018-1534-2.
- [20] R. J. Xu et al., "Micropore formation process during stretching of polypropylene casting precursor film," *Plastics, Rubber and Composites*, vol. 43, no. 8, pp. 257–263, Oct. 2014, doi: 10.1179/1743289814y.0000000100.
- [21] M. Farah and R. E. S. Bretas, "Characterization of i-PP shear-induced crystallization layers developed in a slit die," *Journal of Applied Polymer Science*, vol. 91, no. 6, pp. 3528–3541, Mar. 2004, doi: 10.1002/app.13576.
- [22] W. H. Bednarek, D. Paukszta, M. Szostak, and J. Szymańska, "Fundamental studies on shear-induced nucleation and beta-phase formation in the isotactic polypropylene-effect of the temperature," *Journal of Polymer Research*, vol. 28, Oct. 2021, Art. no. 439, doi: 10.1007/s10965-021-02652-5.
- [23] S. Zhang et al., "Nanocomposite polymer membrane derived from nano TiO<sub>2</sub>-PMMA and glass fiber nonwoven: High thermal endurance and cyclestability in lithium ion battery applications," *Journal of Materials Chemistry A*, vol. 3, no. 34, pp. 17697–17703, Sep. 2015, doi: 10.1039/C5TA02781K.
- [24] H. Kim, V. Guccini, H. Lu, G. Salazar-Alvarez, G. Lindbergh, and A. Cornell, "Lithium ion battery separators based on carboxylated cellulose nanofibers from wood," *ACS Applied Energy Materials*, vol. 2, no. 2, pp. 1241–1250, Feb. 2019, doi: 10.1021/acsaem.8b01797.
- [25] A. Manthiram, "A reflection on lithium-ion battery cathode chemistry," *Nature Communications*, vol. 11, no. 1, Mar. 2020, Art no. 1550, doi: 10.1038/s41467-020-15355-0.